

Impact of the Aggregate Response of Distributed Energy Resources on Power System Dynamics

Taulant Kërçi*, *Student Member, IEEE*, Mel T. Devine†, Mohammed Ahsan Adib Murad*, *Student Member, IEEE*, Federico Milano*, *Fellow, IEEE*

* School of Electrical and Electronic Engineering,
University College Dublin, Ireland
{taulant.kerci, mohammed.murad}@ucdconnect.ie, federico.milano@ucd.ie

† School of Business,
University College Dublin, Ireland
mel.devine@ucd.ie

Abstract—This paper addresses a current concern of the Irish transmission system operator, namely, the impact of aggregated distributed energy resources (DERs) on the dynamic behavior of transmission systems. The aggregation of DERs is done through the virtual power plant (VPP) concept. The paper considers two approaches to operate the VPPs. First, a mixed-integer linear programming (MILP) that optimally schedules the DERs that compose the VPP is presented. The MILP is embedded into a time domain simulator (TDS) by means of co-simulation framework in order to study its impact on the dynamic response of the system. Then, an automatic generation control (AGC) approach is proposed to coordinate the DERs included in the VPP. The case study based on the IEEE 39-bus system serves to illustrate the features and dynamic behaviour of the proposed approaches.

Index Terms—Distributed energy resources, virtual power plant, transmission system, time domain simulation, power system dynamics.

I. INTRODUCTION

The large-scale integration of distributed energy resources (DERs) into power systems allows more electricity generation from renewable energy sources as well as reduces the impact on the environment [1]. However, the penetration of DERs creates additional challenges for transmission system operators (TSOs) mainly due to their uncertain and variable nature as well as the lack of visibility (i.e., mostly connected on the distribution level) [2]. For this reason, it is important to manage DERs in order to better contribute to electricity markets [3], and system operation [1].

A way to address this problem is to make use of the virtual power plant (VPP) concept. A VPP is generally composed of different DERs technologies, including conventional (e.g., gas power plants) and non-conventional (e.g., wind power plants) generating units, storage systems and flexible loads, and operates as a single transmission-connected generator.

In the Irish power system, there are many DERs units that operate as a VPP in the electricity market [4]. EirGrid, the Irish TSO, requires that the power output of a VPP increases

This work was supported by Science Foundation Ireland, by funding Taulant Kërçi, Mel T. Devine and Federico Milano under Grant No. SFI/15/SPP/E3125; Mohammed Ahsan Adib Murad and Federico Milano under Grant No. SFI/15/IA/3074.

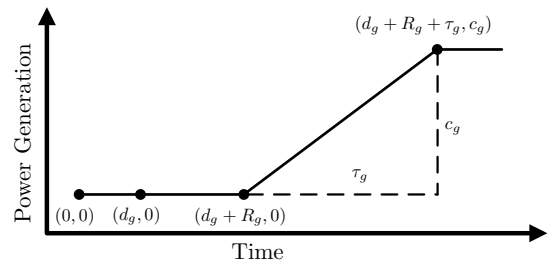


Fig. 1: Power production of a single small generator [6].

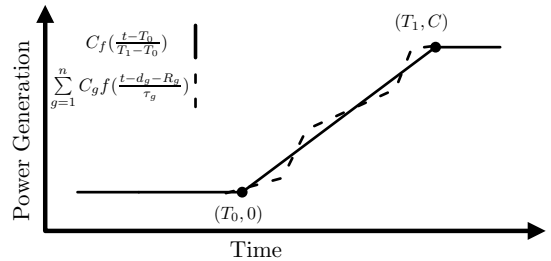


Fig. 2: Power production of a single large power plant (continuous line) and that of a collection of small generators (dashed line) [6].

linearly during the ramp-up time [5]. The TSO does not reward the excess power if the VPP generates more than the agreed linear ramp. On the other hand, the VPP incurs a fine if it is unable to provide the scheduled power [6]. This is a challenge for VPPs as different generators have different characteristics (e.g., different capacity, response and ramping time), and thus the aggregate ramping rate may be non-linear. This problem was raised by a local company to the 141st European Study Group with Industry workshop held in Dublin, Ireland, on June 2018, that was attended by the first two authors [6].

To illustrate the problem faced by the VPPs in the Irish power system, Figs. 1 and 2, show the power production of a single small generator, and the power production of both a single large power plant and that of many small generators, respectively. The points in Fig. 1 have the following meanings:

- $(0, 0)$, is the time when the TSO tells the VPP to go to the maximum production.
- $(d_g, 0)$, is the delay time of the VPP, i.e., how long the VPP takes to send a signal to the g -th generator to start

the production.

- $(d_g + R_g, 0)$, is the time at which the g -th generator transitions from the minimum to the ramping production, and R_g is the response time of the g -th generator of the VPP, i.e. how long such a generator takes to respond to the instruction from the VPP.
- $(d_g + R_g + \tau_g, c_g)$, is the time at which the g -th generator of the VPP transitions from the ramping to the maximum production, where τ_g is the ramping time and c_g corresponds to the maximum capacity of the g -th generator.

The points in Fig. 2 have the following meanings:

- $(T_0, 0)$, is the time when the ramping of the VPP begins.
- (T_1, C) , is the time when the ramping of the VPP stops, where C corresponds to the total capacity of the generators that compose the VPP.

The functions

$$Cf \left(\frac{t - T_0}{T_1 - T_0} \right), \quad (1)$$

$$\sum_{g=1}^n C_g f \left(\frac{t - d_g - R_g}{\tau_g} \right). \quad (2)$$

represent the power generated by a single large power plant (linear), and the total power output of small generators of the VPP (piecewise linear), respectively. A thorough discussion on how to achieve an aggregate ramping rate of the VPP which is as close to linear as possible is given in [6].

Motivated by the discussion above, we address the following research questions: (i) what is the impact of linear aggregate response of a VPP on high voltage transmission grid? (ii) is there any difference between imposing or not imposing such a linear ramping response? and what is the best operation and control of a VPP from the TSO point of view?

To answers these questions, we consider two approaches. First, an optimization problem based on mixed-integer linear programming (MILP) that optimally schedules the small generators of the VPP in order to achieve a linear ramping is presented. The MILP-based VPP is embedded into a time domain simulator (TDS) by means of a recent proposed co-simulation framework, in order to study its impact on the dynamic behaviour of the system. Second, an approach based on automatic generation control (AGC) is proposed and used to coordinate the DERs that form the VPP.

A. Contributions

The contributions of the paper are as follows:

- Study the impact of linear aggregate response of VPPs on the dynamic behaviour of the system and propose a simple yet efficient AGC approach for VPPs.
- Show that at low penetration levels of VPPs, there might be no need to enforce a ramping limit by the TSO.
- Demonstrate that an AGC-based approach leads to a better dynamic performance of the system as compared to that of the VPPs based on MILP scheduling.

B. Paper Organization

The remainder of the paper is organized as follows. Section II describes the mathematical formulation of the VPP based on MILP; the AGC approach; the power system model for transient stability analysis; and the co-simulation framework. Section III discusses the impact of different control approaches and penetration levels of VPPs on the dynamic response of the IEEE 39-bus system. Conclusions and future work directions are given in Section IV.

II. MODELING

A. MILP-based VPP

MILP is commonly utilized by TSOs to solve power system operation (e.g., unit commitment) and planning problems. These analyses are facilitated by the significant improvements of the efficiency and robustness of MILP solvers in recent years [7]. In this work, we use the MILP model proposed in [6] to optimally schedule the single generators of the VPP and obtain a ramping rate that is as close to linear as possible. The mathematical formulation of such a problem is as follows.

$$\min \sum_t (p_{a,t} + K p_{b,t}), \quad (3)$$

such that

$$p_{g,t} \leq C_g, \quad \forall g, t, \quad (4)$$

$$p_{g,t} = p_{g,t-1} + R_g (b_{g,t} - \overline{b_{g,t}}), \quad \forall g, t, \quad (5)$$

$$b_{g,t} \geq b_{g,t-1}, \quad \forall g, t, \quad (6)$$

$$\overline{b_{g,t}} \geq \overline{b_{g,t-1}}, \quad \forall g, t, \quad (7)$$

$$\sum_t (b_{g,t} - \overline{b_{g,t}}) = \tau_g, \quad \forall g, \quad (8)$$

$$\sum_g p_{g,t} + p_{b,t} - p_{a,t} = \frac{t \sum_g C_g}{|\tilde{T}|}, \quad \forall t, \quad (9)$$

$$b_{g,t}, \overline{b_{g,t}} \in \{0, 1\}, \quad \forall g, t, \quad (10)$$

$$p_{g,t}, p_{a,t}, p_{b,t} \geq 0, \quad \forall g, t. \quad (11)$$

where $p_{a,t}$ and $p_{b,t}$ represent continuous variables that model the distances above and below the target linear characteristic at time t , respectively (see Fig. 2). K represents a penalty multiplier when the actual ramping rate is below the target line, i.e., this is needed as the VPP is penalized if it provides less power but that is not true for the other way round. In this work, a value of $K = 10$ is considered. Equations (4) model the capacity limits of single small generators, where $p_{g,t}$ represents the active power generation of the g -th generator at time period t . Equalities (5) model the ramping limits of generating units, where the binary variables $b_{g,t}$ model the status of generating units when they are generating (1 if producing and 0 otherwise), while the binary variables $\overline{b_{g,t}}$ model the status of generating units when they are generating at maximum capacity (1 if true and 0 otherwise). Equations (6) and (7) model the logic of the binary variables. Equations (8) model the generators ramp time (τ_g), i.e. the sum of the differences $b_{g,t} - \overline{b_{g,t}}$ must equal τ_g . Equations (9) model the target ramping line, i.e. $\frac{t \sum_g C_g}{|\tilde{T}|}$, with $|\tilde{T}|$ representing the

total number of time periods. Finally, equations (10) and (11) represent variable declarations.

B. AGC-based VPP

TSOs rely on secondary frequency regulation or AGC to restore the frequency to the nominal value as well as keep the interchange between different areas at the scheduled values [8]. The AGC operates in the time scale of tens of seconds up to tens of minutes and eliminates the steady-state frequency error remained after the primary frequency control [9]. In this work, we consider an AGC scheme that coordinates the DERs that belong to the VPP.

The AGC control scheme considered in this paper is shown in Fig. 3 [8]. For the conventional secondary frequency control, the measured signal $u = \omega_{\text{pilot}}$ is the frequency of a pilot bus of the system, which is then compared to a reference frequency, i.e. $u^{\text{ref}} = \omega^{\text{ref}}$. An integrator block is included to reduce the steady-state error to zero, with K_0 being its gain. Finally, the AGC coordinates each turbine governor (TG) of the generators proportionally to their droop, i.e. R_g/R_{tot} , where $R_{\text{tot}} = \sum_{g=1}^n$.

We propose an AGC scheme for the VPP that instead of regulating the frequency, regulates the total active power of the VPP. With this aim, the signal $u^{\text{ref}} = p_{\text{VPP}}^{\text{ref}}$, i.e., the reference power signal sent by the TSO to the VPP and $u = p_{\text{VPP}}$ is the sum of the measured active power of the DERs included in the VPP.

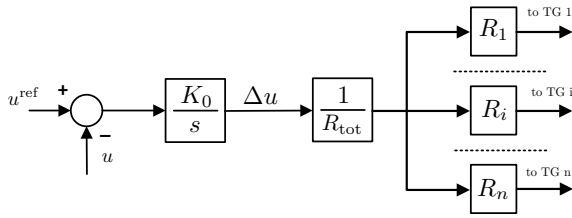


Fig. 3: Basic AGC control scheme for active power regulation of VPPs.

C. Power System Model

Power system dynamics with inclusion of stochastic processes can be modelled as a set of hybrid nonlinear stochastic differential-algebraic equations (SDAEs) [10]:

$$\begin{aligned} \dot{\mathbf{x}} &= \mathbf{f}(\mathbf{x}, \mathbf{y}, \mathbf{u}, \mathbf{z}, \boldsymbol{\eta}) \\ \mathbf{0} &= \mathbf{g}(\mathbf{x}, \mathbf{y}, \mathbf{u}, \mathbf{z}, \boldsymbol{\eta}) \\ \dot{\boldsymbol{\eta}} &= \mathbf{a}(\mathbf{x}, \mathbf{y}, \boldsymbol{\eta}) + \mathbf{b}(\mathbf{x}, \mathbf{y}, \boldsymbol{\eta}) \boldsymbol{\xi}, \end{aligned} \quad (12)$$

where \mathbf{f} , \mathbf{g} are the differential and algebraic equations, respectively; \mathbf{x} , \mathbf{y} , \mathbf{z} are the state, algebraic, and discrete variables, respectively; \mathbf{u} are the inputs, e.g. load forecast and active power schedules; $\boldsymbol{\eta}$ represents stochastic perturbations, e.g. wind speed variations, which are modeled through the last term in (12); \mathbf{a} and \mathbf{b} represent the *drift* and *diffusion* of the stochastic differential equations (SDEs), respectively; and $\boldsymbol{\xi}$ represents the white noise vector.

Equations (12) include the dynamic models of synchronous machines, TGs, automatic voltage regulators, power system stabilizers, wind power plants, AGC, and the discrete model

of VPPs based on MILP scheduling. In particular, TGs are modelled as a conventional droop and a lead-lag transfer function, whereas wind power plants are represented by aggregated models, which implement a 5-th order Doubly-Fed Induction Generator (DFIG) with voltage, pitch angle and MPPT controllers [11].

D. Co-Simulation Framework

Co-simulation allows studying the dynamic behaviour of modern power systems by coupling different sub-domain models, e.g. power systems and electricity markets [12]. Figure 4 shows the structure of the co-simulation framework presented in [13]. Such a framework merges together the model of the sub-hourly stochastic unit commitment (sSCUC), the model of MILP- and AGC-based VPPs, as well as the dynamic model of power systems described in the previous section. A rolling horizon approach is used to feed back the current values of the demand, e.g. $d_{j,t}$, to the sSCUC problem. For space limitations, we do not present here the sSCUC model but the interested reader can find the complete formulation in [14]. The solutions of the sSCUC ($p_{g,t}, \forall g$) and the regulating signals ($R_g \Delta u / R_{\text{tot}}$) generated by the AGC, are utilized to change the power set point of the turbine governors of the power plants.

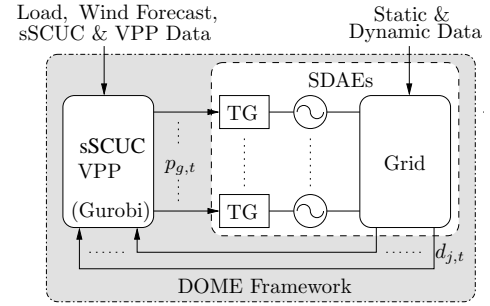


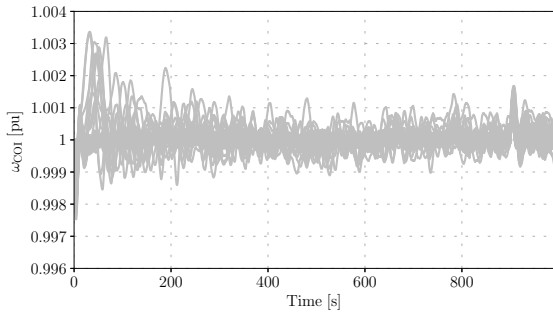
Fig. 4: Co-simulation framework that includes the sSCUC, the dynamic model of the grid and of the DERs that compose the VPP.

III. CASE STUDY

To study the effectiveness and the impact of the VPP operation on the dynamic behaviour of power systems, we consider a modified version of the IEEE 39-bus system [15]. The data of the sSCUC are based on [16], whereas VPP data are taken from [6]. To simulate the VPP, we connect 10 small generators at buses 10-19. In the following, we assume that the VPP is only composed of non-renewable generation, i.e. small gas power plants, as it is the case in the Irish system. The focus is on the first 15 minutes of the planning horizon that is the relevant time window for the aggregated response of DERs. Furthermore, in order to create a realistic scenario that represents the current situation in the Irish power system, the real-world data of the VPP made available by EirGrid are used in the simulations below [4]. Based on these data, the VPP capacity with respect to the total generation capacity is about 4.3%. For consistency, in the first of the case study, we thus use a VPP/grid capacity ratio of 5%.

TABLE I: DERs data for the MILP-based VPP

Generator	Capacity (MW)	Response time (min)	Ramping time (min)
1	0.68	2.73	13.17
2	3.16	6.13	49.61
3	3.74	10.71	39.00
4	1.68	6.91	34.51
5	4.32	1.78	35.49
6	3.89	11.34	28.52
7	1.74	11.23	43.04
8	4.92	9.00	15.14
9	1.02	1.51	4.17
10	4.80	9.48	33.20


 Fig. 5: ω_{COI} for 5% VPP penetration with ramping constraint.

The modeling of wind power uncertainty and volatility within the sSCUC model, as well as the modeling of stochastic nature of wind based on SDEs is the same as in [14]. Moreover, 25% wind penetration level is considered, where the wind generation is given by wind power plants connected to buses 20-23.

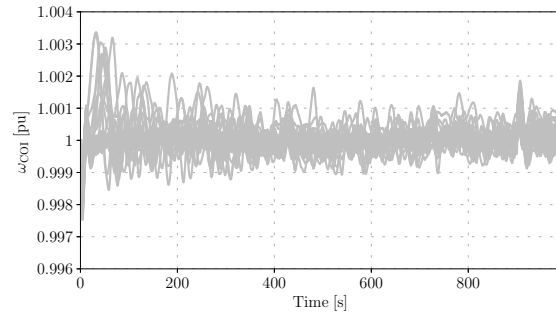
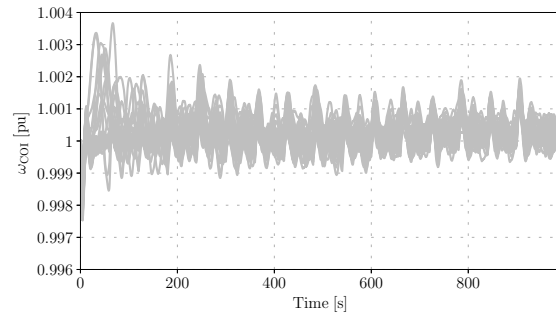
The study carries out Monte Carlo time domain simulations and 50 simulations are solved for each scenario. The MILP problem (3)-(11) and the sSCUC model are implemented in the Python language and solved using Gurobi [17], while all simulations are obtained using DOME, a Python-based software tool for power system dynamic analysis [18].

A. 5% Penetration of VPPs

In this scenario, only VPPs with MILP scheduling are considered. Table I shows relevant data of the 10 DERs that form the VPP [6]. The total capacity of these generators is 29.95 MW, which means that they represent around 5% of the total generation in [16] (during the first 15 minutes of the planning horizon). The time period t used in the simulations is 1 minute. Thus, the VPP provides 29.95 MW at the end of the 15 minute period. Moreover, we assume that the system operator requires this power to increase linearly with respect of time.

1) *VPP with ramping constraints*: Figure 5 depicts the trajectories of the frequency of the center of inertia (ω_{COI}) and shows that there are significant frequency oscillations at the beginning of the planning horizon due to the ramping of generators. The value of the standard deviation of the frequency is $\sigma_{COI} = 0.000556$ pu(Hz).

2) *VPP without ramping constraints*: In this scenario, we discuss whether removing the ramping limit of VPP leads to


 Fig. 6: ω_{COI} for 5% VPP penetration without ramping constraint.

 Fig. 7: ω_{COI} for 20% VPP penetration with ramping constraint.

a worse dynamic behaviour of the system. This will allow us to check the effect of the ramping limit enforced by the TSO. Figure 6 shows the trajectories of ω_{COI} . Compared to the previous case (Fig. 5), where ramping limits are enforced, the value of σ_{COI} is 0.000601 pu(Hz) and, hence, there is no significant difference on the dynamic behaviour of the system. Thus, it appears that, with a low VPP penetration level, there might be no need to enforce a ramping limit on VPPs.

B. 20% Penetration of VPPs

This scenario is relevant for microgrids and/or future grids such as the Irish system with high penetration of DERs.

1) *VPP with ramping constraints*: Figure 7 depicts the trajectories of the ω_{COI} for the case when the ramping limit is enforced. With a standard deviation $\sigma_{COI} = 0.000571$ pu(Hz), frequency variations are slightly higher compared to the 5% penetration scenario (Fig. 5).

2) *VPP without ramping constraints*: Similar to Subsection III-A2, we check the importance of the ramping limit of the VPP. Figure 8 shows the trajectories of the ω_{COI} for the case when the ramping limit is not enforced. This leads to a worse dynamic behaviour of the system compared to Fig. 7. In this case, the value of the σ_{COI} is 0.000645 pu(Hz). Hence, increasing the penetration levels of VPPs, while increasing their impact on the system, does not constitute a stability issue for the system.

C. AGC-based VPP

This section discusses the performance of the AGC described in Section II-B and assumes a 20% penetration of VPPs. The gain of the AGC is set to $K_0 = 50$. Figure 9 shows

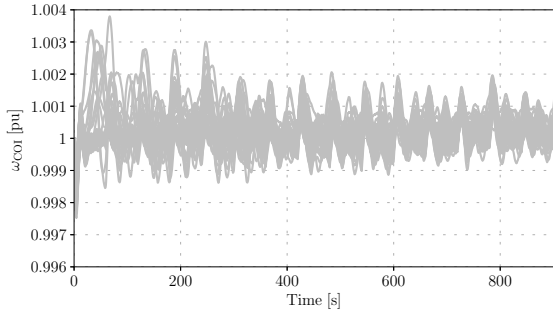


Fig. 8: ω_{COI} for 20% VPP penetration without ramping constraint.

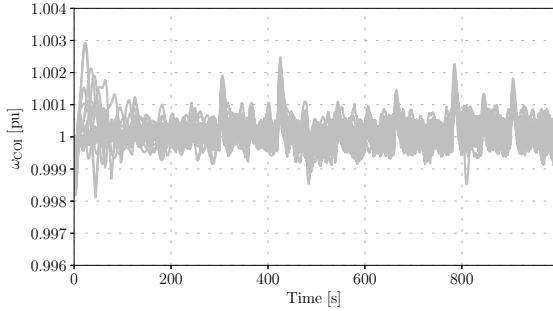


Fig. 9: ω_{COI} for the AGC-based VPP with 20% penetration.

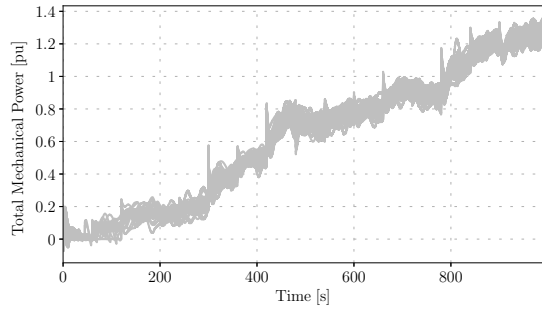


Fig. 10: Total mechanical power of 10 relevant machines of the AGC-based VPP.

the trajectories of ω_{COI} for 15 minutes. The frequency variations are significantly lower, i.e. $\sigma_{COI} = 0.000459$ pu(Hz), compared to those shown in Fig. 7. This is due to the fact that the AGC coordinates the DERs in such a way that they start ramping up all at the same time and then smoothly increase their generation (see Fig. 10). From a system operator point of view, thus, the AGC-based VPP is preferable with respect to the conventional scheduling based on a MILP problem.

IV. CONCLUSIONS

This paper studies the impact of a linear aggregate operation of DERs on the dynamic response of a transmission system. With this aim, the paper considers two approaches, namely, an optimization problem based on MILP and an AGC that coordinate the DERs to achieve a linear ramping. Both approaches are simulated through a co-simulation platform recently developed by the first and fourth authors.

The case study shows that at a low penetration level of VPPs (5%) there is effectively no relevant difference on the dynamic

performance of the system when imposing the ramping limit or not. For a higher penetration level of the VPP (20%), while frequency variations remain relatively small, ramping limit leads to a slightly better dynamic behaviour of the system. A comparison of both approaches with respect to long-term frequency deviations shows that an AGC is to be preferred compared to scheduling based on an optimization problem as it leads to lower frequency variations of the system.

Future work will focus on applying the proposed methods to microgrids with a high penetration of DERs.

REFERENCES

- [1] D. Pudjianto, C. Ramsay, and G. Strbac, "Virtual power plant and system integration of distributed energy resources," *IET Renewable Power Generation*, vol. 1, no. 1, pp. 10–16, March 2007.
- [2] R. Quint, L. Dangelmaier, I. Green, D. Edelson, V. Ganugula, R. Kaneshiro, J. Pigeon, B. Quaintance, J. Riesz, and N. Stringer, "Transformation of the grid: The impact of distributed energy resources on bulk power systems," *IEEE Power and Energy Magazine*, vol. 17, no. 6, pp. 35–45, Nov 2019.
- [3] S. Ghavidel, L. Li, J. Aghaei, T. Yu, and J. Zhu, "A review on the virtual power plant: Components and operation systems," in *2016 IEEE International Conference on Power System Technology (POWERCON)*, Sep. 2016, pp. 1–6.
- [4] EirGrid, "Tomorrow's Energy Scenarios 2017," 2017. [Online]. Available: <http://www.eirgridgroup.com/site-files/library/EirGrid/EirGrid-Tomorrows-Energy-Scenarios-Report-2017.pdf>
- [5] —, "EirGrid Grid Code. Version 8," 2019. [Online]. Available: <http://www.eirgridgroup.com/site-files/library/EirGrid/Grid-Code.pdf>
- [6] P. Beagon, M. D. Bustamante, M. T. Devine, S. Fennell, J. Grant-Peters, C. Hall, R. Hill, T. Kerci, and G. O'Keefe, "Optimal scheduling of distributed generation to achieve linear aggregate response," *Proceedings from the 141st European Study Group with Industry*, 2018, available at: <http://www.maths-in-industry.org/miis/758/>.
- [7] G. Morales-España, J. M. Latorre, and A. Ramos, "Tight and compact milp formulation for the thermal unit commitment problem," *IEEE Transactions on Power Systems*, vol. 28, no. 4, pp. 4897–4908, Nov 2013.
- [8] P. Kundur, *Power System Stability and Control*. New York: McGraw-Hill, 1994.
- [9] F. Milano, F. Dörfler, G. Hug, D. J. Hill, and G. Verbič, "Foundations and challenges of low-inertia systems (invited paper)," in *Power Systems Computation Conference (PSCC)*, Dublin, Ireland, Jun 2018, pp. 1–25.
- [10] F. Milano and R. Zárate-Miñano, "A systematic method to model power systems as stochastic differential algebraic equations," *IEEE Transactions on Power Systems*, vol. 28, no. 4, pp. 4537–4544, Nov 2013.
- [11] F. Milano, *Power System Modelling and Scripting*. London: Springer, 2010.
- [12] P. Palensky, A. A. Van Der Meer, C. D. Lopez, A. Joseph, and K. Pan, "Cosimulation of intelligent power systems: Fundamentals, software architecture, numerics, and coupling," *IEEE Industrial Electronics Magazine*, vol. 11, no. 1, pp. 34–50, March 2017.
- [13] T. Kërçi and F. Milano, "A framework to embed the unit commitment problem into time domain simulations," in *IEEE International Conference on Environment and Electrical Engineering*, June 2019, pp. 1–5.
- [14] T. Kërçi, J. S. Giraldo, and F. Milano, "Analysis of the Impact of Sub-Hourly Unit Commitment on Power System Dynamics," *Submitted to the Int. J. of Electric Power & Energy Systems*, September 2019, available at: <http://faraday1.ucd.ie/archive/papers/suctds.pdf>.
- [15] Illinois Center for a Smarter Electric Grid (ICSEG), "IEEE 39-Bus System," URL: <http://publish.illinois.edu/smartergrid/ieec-39-bus-system/>.
- [16] M. Carrión and J. M. Arroyo, "A computationally efficient mixed-integer linear formulation for the thermal unit commitment problem," *IEEE Transactions on Power Systems*, vol. 21, no. 3, pp. 1371–1378, Aug 2006.
- [17] L. Gurobi Optimization, "Gurobi optimizer reference manual." [Online]. Available: <http://www.gurobi.com>
- [18] F. Milano, "A Python-based software tool for power system analysis," in *IEEE PES General Meeting*, Vancouver, BC, July 2013.